Local Lattice Dynamics and the Origin of the Relaxor Ferroelectric Behavior

W. Dmowski,[1] S. B. Vakhrushev,[2] I.-K. Jeong,[3] M. P. Hehlen,[4] F. Trouw,[4] and T. Egami[1,5,6]

[1]*Department of Materials Science and Engineering, University of Tennessee, Knoxville, Tennessee 37996, USA*
[2]*Ioffe Physico-Technical Institute, St. Petersburg, 194021, Russia*
[3]*Department of Physics, Pusan National University, Busan, Korea*
[4]*LANSCE, Los Alamos National Laboratory, Los Alamos, New Mexico 87545, USA*
[5]*Department of Physics and Astronomy, University of Tennessee, Knoxville, Tennessee 37996, USA*
[6]*Oak Ridge National Laboratory, Oak Ridge, Tennessee 37831, USA*
(Received 12 December 2007; published 4 April 2008)

Relaxor ferroelectricity is observed in many strongly disordered ferroelectric solids. However, the atomistic mechanism of the phenomenon, particularly at high temperatures, is not well understood. In this Letter we show the local lattice dynamics as the origin of relaxor ferroelectricity through the first use of the dynamic pair-density function determined by pulsed neutron inelastic scattering. For a prototypical relaxor ferroelectric, $Pb(Mg_{1/3}Nb_{2/3})O_3$, we demonstrate that the dynamic local polarization sets in around the so-called Burns temperature through the interaction of off-centered Pb ions with soft phonons, and the slowing down of local polarization with decreasing temperature produces the polar nanoregions and the relaxor behavior below room temperature.

DOI: 10.1103/PhysRevLett.100.137602 PACS numbers: 77.80.−e, 77.22.Ej, 77.22.Gm, 77.84.Dy

Strongly disordered ferroelectric materials called relaxor ferroelectrics are attractive for various applications because of their exceptionally high dielectric and piezoelectric responses over a wide range of temperature [1,2]. They show a strong and broad peak in the dielectric constant as a function of temperature, with the peak temperature, T_f, being frequency-dependent. Above T_f they show high dielectric response that is little dependent on frequency. This high dielectric response is considered to be due to formation of polar nanoregions (PNRs), mesoscopic regions with local polarization [3–5]. But optical measurements suggest that local ferroelectric activity is present up to a much higher temperature, known as the Burns temperature, T_d [6]. Judged from the frequency dependence of dielectric constant, the frequency range of ferroelectric polarization dynamics at such high temperatures has to be comparable to that of lattice dynamics (THz). Indeed, anomalous phonon behavior called the "phonon waterfall" has been observed by inelastic neutron scattering measurement, at temperatures below T_d and above T_f, while regular phonon dispersion is observed at $T > T_d$ and $T < T_f$ [7–9]. Between T_d and T_f a portion of the phonon dispersion becomes overdamped, implying strong effect of disorder and localization of lattice dynamics.

But the atomistic mechanism to produce these unique dynamics and temperature dependence of relaxor ferroelectrics is not well understood. In this Letter we report the direct observation of the dynamic local polarizations in a prototypical relaxor ferroelectric, $Pb(Mg_{1/3}Nb_{2/3})O_3$ (PMN), and show how the local lattice dynamics and its evolution with temperature will produce the relaxor ferroelectric behavior. PMN has a nominally cubic perovskite structure, but randomness in the A-site occupation by Nb^{5+} and Mg^{2+} results in the strongly distorted local structure [10] and apparently in the relaxor behavior. PMN has T_f of about 230 K at low frequencies (~10 Hz), increasing to 320 K at 1 GHz [11] with T_d of 635 K. In order to observe such local lattice dynamics directly, we have carried out inelastic neutron scattering measurements to determine the dynamical structure factor $S(Q, E)$ over a wide range in Q and E, where Q is the scattering vector (momentum transfer) and $E = \hbar\omega$ is the energy transfer. Since phonons are overdamped, in order to observe local lattice dynamics the results were Fourier transformed over Q to examine the real-space dynamic correlation. The measurements were done with the pulsed neutron time-of-flight method using the PHAROS spectrometer at LANCE, Los Alamos National Laboratory, on a powder PMN sample of about 100 grams provided by J.-S. Park and K.-S. Hong of School of Material Science and Engineering, Seoul National University. The incoming neutron beam was monochromatized by a mechanical chopper, and scattered neutrons were detected as a function of time by an array of position sensitive detectors placed over a wide range of scattering angles up to 160°. The measurements were performed at temperatures 680 K, 590 K ($\sim T_d$), 450 K, 300 K, 230 K ($\sim T_f$), and 35 K. High incident energy of 250 meV was selected to access a wide range of Q (up to about 20 $Å^{-1}$) and E space. Since the inelastic neutron scattering cross section is small, we had to continue the measurement for as long as two days at each temperature.

Figure 1 shows $S(Q, E)$ of Ni powder measured at $T = 300$ K 1(a) and of PMN at $T = 450$ K 1(b), with the intensity shown by color. The energy resolution at $E = 0$ is about 4 meV. Energy is transferred from a neutron to the sample for $E > 0$ (energy gain) and from the sample to a neutron for $E < 0$ (energy loss). Since the sample is polycrystalline, all orientations are averaged, so that at

 © 2008 The American Physical Society

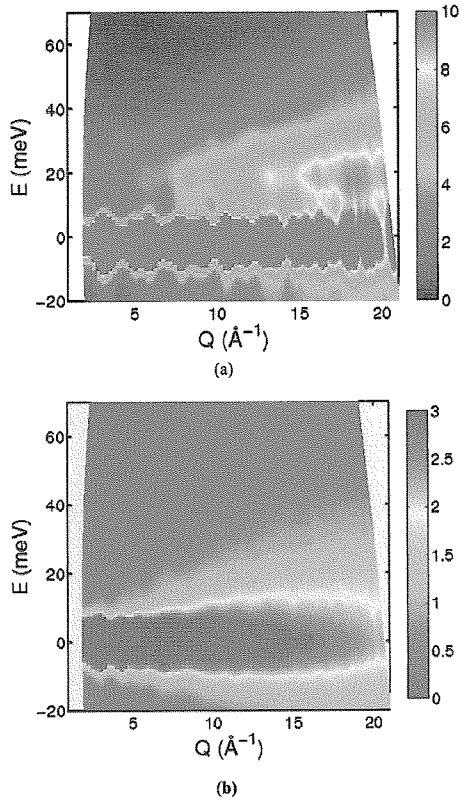

FIG. 1 (color). Dynamic structure factor $S(Q, E)$ of polycrystalline Ni at $T = 300$ K (a), and of PMN at $T = 450$ K (b). Color scheme indicates the intensity.

high Q values many Brillouin zones overlap, making $S(Q, E)$ rather featureless. Even for Ni only around the (1 1 1) Bragg peak at 3.1 Å^{-1} acoustic phonon branches are barely seen. $S(Q, E)$ of PMN is even more featureless, because PMN is more complex than Ni and is disordered. A rapid decrease in the elastic ($E = 0$) intensity with Q is due to the strong Debye-Waller factor. In order to extract the physical meanings of such featureless data, we apply Fourier transformation to them. The Fourier transform of the elastic component, $S(Q, 0)$, describes the static pair-density function (PDF) of the time-averaged structure over Q, $\rho(r, E = 0)$, i.e., the autocorrelation function of the time-averaged atomic density [12]. For a perfect crystal $\rho(r, 0)$ comprises many Gaussian peaks of which position corresponds to the distance between the crystallographic sites and the width to the amplitude of lattice vibration. On the other hand, if we integrate $S(Q, E)$ over energy E before Fourier transformation, we obtain the PDF of the instantaneous or snapshot (equal time) atomic positions [12]. The PDF determined by x-ray scattering is of this type, since the resolution of x-ray scattering, conventionally 1–10 eV, is much larger than the phonon energy and effectively integrates over all the phonon energies.

The Fourier transform of $S(Q, E)$ over Q and E is known as the van Hove function, $G(r, t)$ [13], and the Fourier transform only over E, $I(Q, t)$, is called the intermediate function [14]. We define the Fourier transform of $S(Q, E)$ over Q, $\rho(r, E)$, as the dynamic PDF (DPDF) [12,15]. It describes the atomic correlation, or the distribution of atomic distances over time, at the angular frequency of $\omega = E/\hbar$. As an example, we show the Fourier transform of $S(Q, E)$ shown in Fig. 1(a), the DPDF of polycrystalline Ni, in Fig. 2(a). We also show in Fig. 2(b) the simulated DPDF obtained by Fourier transforming the $S(Q, E)$ calculated from the phonon dispersion for Ni [16] including the experimental resolution of Q and E and the cutoff at $Q_{\max}$. They are in good agreement, demonstrating that the DPDF can be experimentally determined by pulsed neutron scattering with sufficient accuracy. Interestingly both show that the peak due to the nearest Ni-Ni distance at 2.5 Å splits into two subpeaks at 2.22 and 2.73 Å, around 33 meV. The period of the termination error ($2\pi/Q_{\max} = 0.31$ Å) is not commensurate with the peak splitting, indicating that the peak splitting is real. It should be noted that there is a sharp van Hove singularity in the phonon dispersion of Ni at this energy [16]. As will be discussed elsewhere, the DPDF catches only the local or semilocal phonons that originate from the flat portion of the phonon dispersion, while regular phonons with strong dispersion will hardly be observed by this technique. Thus, this technique complements the conventional method and focuses only on local

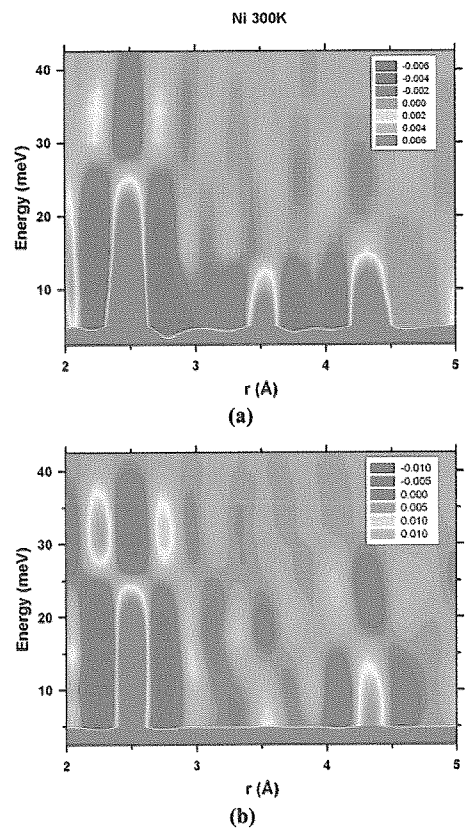

FIG. 2 (color). (a) Dynamic PDF of polycrystalline Ni measured at 300 K, and (b) DPDF theoretically calculated for polycrystalline Ni at 300 K.

phonons that are difficult to study with the conventional method.

Figure 3 shows the DPDF for PMN measured at $T = 450$ K. At low energies the first peak at 2 Å is due to the (Nb, Mg)-O distances, and the second peak at 2.8 Å describes the O–O as well as Pb–O distances in the average perovskite structure. Above ~15 meV (~4 THz), however, a strong peak shows up at 2.4 Å. The position of this peak agrees with the short Pb–O distances that occur as a result of Pb off-centering in the cage made of 12 oxygen ions [17]. Pb^{2+} is likely to be off-centered in the direction with more Mg^{2+} ions than Nb^{5+} ions, because Nb ions make it more difficult for oxygen ions to form covalent bonds with Pb [18]. This extra peak must indicate dynamic off-centering of Pb in the PbO_{12} cage. Also the peak at 3.4 Å seen at low frequencies splits into two, at 3.2 and 3.5 Å, also above 15 meV. This peak corresponds to the Pb-(Mg, Nb) distances, so the splitting of this peak also indicates local Pb off-centering against the Mg/Nb sublattice [19]. Thus the DPDF at 450 K shows the presence of *dynamic* local polarization of Pb and O at this temperature with the characteristic frequency of about 4 THz, even though there is no static polarization.

When we compare the DPDF at different temperatures, we find that the temperature evolution is strongly frequency dependent. While measurements were performed only at six temperatures, we chose to display the results as a two-dimensional plot, since it makes it much easier to see what is happening. Consequently, we do not claim detailed interpolations of the temperature dependence to be accurate, for steps smaller than the actual measurements. Figure 4(a) shows the temperature evolution of the static PDF, $\rho(r, 0)$, within the resolution of the present experiment (4 meV = 1 THz). It is clear that the local Pb polarizations represented by the three split peaks of Pb–O correlation at 2.4, 2.8, and 3.3 Å disappear above $T_p \sim 300$ K. On the other hand, Fig. 4(b) shows the DPDF integrated from 10 to 20 meV as a function of temperature.

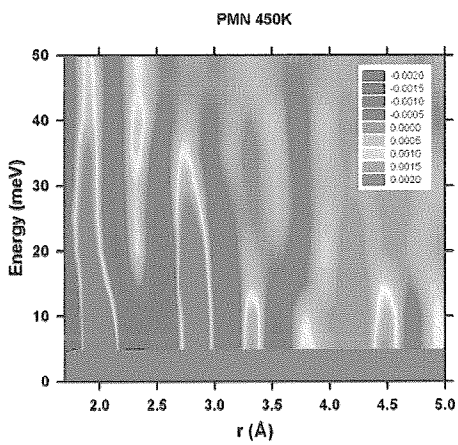

FIG. 3 (color). Dynamic PDF of PMN at 450 K. See text for interpretation.

The satellites of the 2.8 Å Pb–O peak at 2.4 and 3.3 Å extend to higher temperatures than in the static PDF, disappearing only around 600 K, close to the Burns temperature (635 K). The twin peaks at 3.3 and 3.7 Å at low temperatures that correspond to the split Pb-(Mg, Nb) peaks are joined at 3.5 Å at the highest temperature (680 K), with the split disappearing also around 600 K.

It should be noted that the temperature T_p, up to which low frequency polarization is present, is between T_f and T_d. This result is consistent with our earlier total PDF measurements [20,21], which show that the local Pb off-centering and local rhombohedral distortion occur below 300 K. The total PDF measurement is done in the energy-integrated mode, but because of the Placzek shift in Q [22] its energy window is effectively limited [12]. This measurement suggests that the effective energy window is less than 10 meV. Thus, there is *the third* temperature scale in the relaxor ferroelectrics in addition to T_f and T_d; the PNRs are formed below T_p, whereas between T_p and T_d local polarizations are dynamic and are less correlated with little or no rhombohedral distortion. It is interesting to note that T_p is close to the temperature, T_f^{∞} (~350 K), where the low temperature ferroelectric relaxation times extrapolate to phonon frequencies, and T_0 (~340 K) where the intensity of the softening phonon diverges in extrapolation from high temperatures [23]. It is also not far from the temperature (~400 K) where the elastic diffuse neutron scattering intensity disappears and the intensity of the quasielastic scattering becomes maximum [24].

The energy of the soft phonon branches involving Pb–O displacements is about 5–15 meV when the waterfall behavior is observed [8,23], a similar energy range where we see anomalies in Figs. 3 and 4(b). This coincidence suggests that the resonance between the local dynamic off-centering of Pb ions and these soft phonons produces the dynamic short-range correlation in polarization, resulting in the formation of a local polarization cloud at temperatures below T_d. This resonance between the local polar moment and the soft phonons was modeled in a recent calculation [25]. It also must be the origin of the waterfall behavior; long wave phonons are scattered by the local polarization clouds, while there are other interpretations of the waterfall behavior [26,27]. Below T_p dynamic local polarizations slow down sufficiently to form PNRs with local rhombohedral distortion. The behavior of relaxor ferroelectric solids in the radio-frequency range originates from the interaction among PNRs that may be described in terms of the random fields [4,5].

As demonstrated above, the measurement of the dynamic PDF resolved a long-standing question regarding the atomic origin of the formation of dynamic polar nanoregions, and facilitated the understanding of the relaxor ferroelectric behavior at the atomic level. While the lattice dynamics of highly crystalline solids is well characterized by phonons, in strongly disordered systems phonons are localized and are difficult to observe by conventional

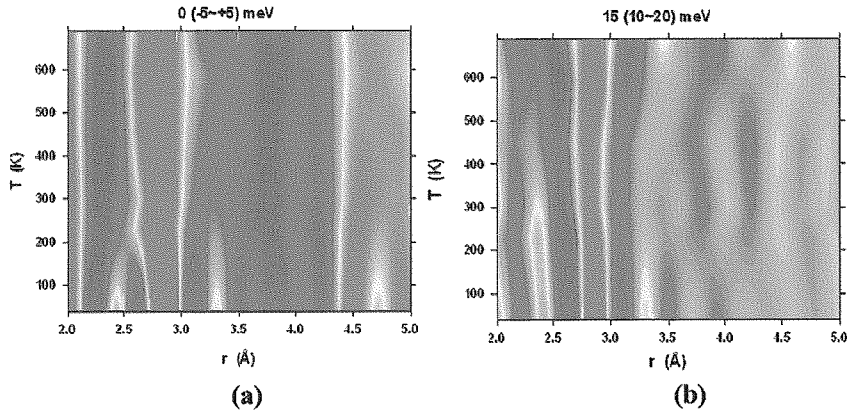

FIG. 4 (color). Temperature dependence of the dynamic PDF of PMN, (a) at $E = 0$ (integrated from -5 meV to $+5$ meV), (b) at $E = 15$ meV (integrated from 10 meV to 20 meV). See text for interpretation.

methods. The DPDF technique described here can be applied to the study of such systems and has a potential to solve many difficult problems involving local dynamics, such as local atomic dynamics in liquids, glasses, and nanoclusters, certain types of chemical reaction, atomic transport in fast ionic conductors, and local spin dynamics in disordered magnets or molecular magnets. As more powerful pulsed neutron sources, such as the Spallation Neutron Source (SNS), become available, this technique can become the technique of choice for the study of local lattice and local spin dynamics.

The authors gratefully acknowledge A. Bussmann-Holder, A. R. Bishop, W. Kleemann, and P. Gehring for useful and insightful discussions and Jiao Lin for help in the DPDF simulation of nickel. This work at the University of Tennessee was supported by the National Science Foundation, No. DMR0602876, and at Oak Ridge National Laboratory by the Laboratory Directed Research and Development Program of Oak Ridge National Laboratory, managed by UT-Battelle, LLC, for the U.S. Department of Energy under Contract No. DE-AC05-00OR22725. This work benefited from the use of PHAROS at the Lujan Center at Los Alamos Neutron Science Center, funded by DOE Office of Basic Energy Sciences and Los Alamos National Laboratory funded by Department of Energy under Contract No. W-7405-ENG-36.

[1] *Ferroelectrics and Related Materials*, edited by G. A. Smolensky (Gordon and Breach, New York, 1981).
[2] L. E. Cross, Ferroelectrics **76**, 241 (1987).
[3] D. Viehland, S. J. Jang, L. E. Cross, and M. Wuttig, Phys. Rev. B **46**, 8003 (1992).
[4] V. Westphal, W. Kleemann, and M. D. Glinchuk, Phys. Rev. Lett. **68**, 847 (1992).
[5] R. Pirc and R. Blinc, Phys. Rev. B **60**, 13470 (1999).
[6] G. Burns and B. A. Scott, Solid State Commun. **13**, 423 (1973).
[7] P. M. Gehring, S. Wakimoto, Z.-G. Ye, and G. Shirane, Phys. Rev. Lett. **87**, 277601 (2001).
[8] S. Wakimoto, C. Stock, R. J. Birgeneau, Z.-G. Ye, W. Chen, W. J. L. Buyers, P. M. Gehring, and G. Shirane, Phys. Rev. B **65**, 172105 (2002).
[9] C. Stock, R. J. Birgeneau, S. Wakimoto, J. S. Gardner, W. Chen, Z.-G. Ye, and G. Shirane, Phys. Rev. B **69**, 094104 (2004).
[10] T. Egami, H. D. Rosenfeld, B. H. Toby, and A. Bhalla, Ferroelectrics **120**, 11 (1991).
[11] V. Bovtun, S. Kamba, A. Pashkin, M. Savinov, P. Samoukhina, J. Petzelt, I. Bykov, and M. Glinchuk, Ferroelectrics **298**, 23 (2004).
[12] T. Egami and S. J. L. Billinge, *Underneath the Bragg Peaks: Structural Analysis of Complex Materials* (Pergamon Press, Elsevier Ltd., Oxford, 2003).
[13] L. van Hove, Phys. Rev. **95**, 249 (1954).
[14] That is, W. Marshall and S. W. Lovesey, *Theory of Thermal Neutron Scattering* (Clarendon Press, Oxford, 1971).
[15] R. J. McQueeney, Phys. Rev. B **57**, 10560 (1998).
[16] R. J. Birgeneau, J. Cordes, G. Dolling, and A. D. B. Woods, Phys. Rev. **136**, A1359 (1964).
[17] T. Egami, W. Dmowski, M. Akbas, and P. K. Davies, AIP Conf. Proc. **436**, 1 (1998).
[18] I. Grinberg and A. M. Rappe, Phys. Rev. B **70**, 220101(R) (2004).
[19] W. Dmowski, M. K. Akbas, P. K. Davies, and T. Egami, J. Phys. Chem. Solids **61**, 229 (2000).
[20] T. Egami, E. Mamontov, W. Dmowski, and S. B. Vakhrushev, AIP Conf. Proc. **677**, 48 (2003).
[21] I.-K. Jeong, T. W. Darling, J. K. Lee, Th. Proffen, R. H. Heffner, J. S. Park, K. S. Hong, W. Dmowski, and T. Egami, Phys. Rev. Lett. **94**, 147602 (2005).
[22] G. Placzek, Phys. Rev. **86**, 377 (1952).
[23] S. B. Vakhrushev and S. M. Shapiro, Phys. Rev. B **66**, 214101 (2002).
[24] H. Hiraka, S.-H. Lee, P. M. Gehring, G. Xu, and G. Shirane, Phys. Rev. B **70**, 184105 (2004).
[25] A. Bussmann-Holder, A. R. Bishop, and T. Egami, Europhys. Lett. **71**, 249 (2005).
[26] C. Stock, D. Ellis, I. P. Swainson, G. Xu, H. Hiraka, Z. Zhong, H. Luo, X. Zhao, D. Viehland, R. J. Birgeneau, and G. Shirane, Phys. Rev. B **73**, 064107 (2006).
[27] J. Hlinka, S. Kamba, J. Petzelt, J. Kulda, C. A. Randall, and S. J. Zhang, Phys. Rev. Lett. **91**, 107602 (2003).